Different Aspects of the Effects of Liquefaction-Induced Lateral Spreading on Piles, Physical Modelling

Theme Lecture to be presented in PBD 2022

S. Mohsen Haeri
smhaeri@sharif.edu

Abstract

Devastating pile failures due to liquefaction induced lateral spreading during or after major earthquakes in gently sloping ground or level grounds with free end, especially the pile foundations located under structures in or near ports and harbors, have been observed and studied for decades. Many physical and numerical modellings have been implemented or developed to study and understand the insight into different aspects of this phenomenon. In this regard, 1-g shake table and N-g dynamic centrifuge tests using both rigid box and laminar shear box have been implemented to physically model the problem and measure the parameters that may affect the impact of lateral spreading on deep foundations. A number of countermeasures have also been examined for tackling this problem. In this paper and theme lecture, the author tries to describe shortly the physical modelling researches and studies that have been conducted by him and his coworkers on this subject in more than a decade, and discuss the various parameters that are involved in physical modelling for studying the behavior of pile foundations subjected to liquefaction induced lateral spreading. A number of limitations involved in such physical modellings are also mentioned and some solutions to the involved challenges are discussed as well.

Keywords: Physical Modelling, 1-g Shake Table Test, Lateral Spreading, Liquefaction, Pile foundations, Countermeasure.

1 Introduction

During past earthquakes, many important structures supported on pile foundations have been subjected to severe damages due to liquefaction induced lateral spreading. Lateral displacements associated with lateral spreading can be up to several meters which consequently can impose substantial kinematic forces to pile foundations, causing extensive damages. Several observations have been reported during past earthquakes in this regard, among which the 1964 Niigata, Japan, the 1983 Nihonkai-Chubu, Japan, the 1989 Loma Prieta, USA, the 1995 Kobe, Japan, the 2001 Bhuj, India and the 2010 Port-au-Prince, Haiti earthquakes are among the most destructive ones [1-7]. Damaged piles in these earthquakes revealed that effects of lateral spreading on deep foundations has not been fully understood and therefore several studies have been undertaken by researchers especially in the last two decades. Design codes also were prepared for design of pile foundations against lateral spreading. A simple and efficient method in this respect was suggested by JRA (2002) [8] for pile design against lateral spreading, based on the observations and lessons learned from Kobe 1995 Earthquake. Although the method proposed by JRA (2002) [8] is a very straightforward and useful tool for design of piles against lateral

spreading, however, it does not give an insight into many aspects of this problem, such as the effect of the position of piles in a pile group. Physical and numerical modelling, however, are two powerful tools for studying the soil-pile systems. In this respect, many studies implementing physical modelling have been performed to investigate the response of piles to lateral spreading [9-20], however, a comprehensive method for design of piles against lateral spreading is yet in need of more experiments and numerical studies. Mitigation of liquefaction-induced lateral spreading hazard on present piles in liquefiable sloping grounds has been a concern for practitioners and researchers. In this regard using stone columns and micro piles are among those methods. Seed and Booker [21] were the first researchers who investigated the effectiveness of stone columns for mitigation of liquefaction. However, Kavand et al. [22, 23] were the first researchers who conducted a series of shake table experiments to study the effectiveness of stone columns and micropiles to countermeasure the effects of lateral spreading on 3×3 flexible and stiff pile groups in a gently sloping ground. They found that stone columns can effectively reduce the kinematic bending moments due to lateral spreading in flexible piles up to a particular level of earthquake magnitude. However, they found that stone columns are ineffective in reducing the effect of lateral spreading on piles in other conditions. Also their test results using picropiles as a mitigation measure showed that the micropiles were not able to reduce effectively the bending moments in the piles while it was able to reduce lateral soil pressures exerted by non-liquefiable crust on the upslope piles of the group. Haeri et el. [24] also conducted two shake table experiments to investigate the efficacy of stone column technique as a mitigation method against liquefaction-induced lateral spreading on two 2×2 pile groups in a laminar shear box. Their results illustrate that stone column technique significantly decreassed lateral displacemnts in the free field and bending moments in the piles, while increased the accelearions in the pile caps and rate of dissipation of excess pore water pressure in the liquefiable layer. All other researchers, e.g. [25-28] used numerical modelling to study the effectiveness of stone columns as remediation measure against the effects of lateral spreading on piles.

In the present paper, the effects of liquefaction-induced lateral spreading on single piles and pile groups which studied by physical modelling in various conditions are discussed. Also efficacy of some methods to mitigate the impact of lateral spreading on piles are evaluated by physical modelling.

2 Characteristics of Physical Modellings of Piles Subjected to Lateral Spreading

Overall, 16 large scale physical models have been constructed and tested in a long run of studies by the author and his coworkers at Sharif University of Technology (SUT) to investigate various aspects of the response of the piles to lateral spreading. For this purpose, shake table facility of Earthquake Engineering Research Center of SUT has been employed. SUT shaking table is a 4m×4m, 3DOFS facility, capable of taking vertical loads up to 300 kN with actuators capacities of 1×500 kN in longitudinal direction and 2×200 kN in transversal direction, and a maximum base acceleration of 2g and a maximum frequency of 50Hz. The first part of this research started in 2009 by design and construction of a rigid box with a transparent side with which 10 large scale tests were carried out and completed in 2013. The results of some of these tests

have been reported and published so far [9, 11, 14, 16-17, 22-23] and results of a number of tests have not been published yet. The dimensions of the rigid container (box) is 3.5m long, 1.0m wide and 1.5m high. Two Plexiglas windows were provided in one side of the container to be able to view and measure the soil lateral movements by PIV method. As the box was long enough in the direction of lateral spreading, and lateral spreading is rather kinematic in nature, it was assumed that the rigid boundary condition in this study could have minimum effects on the results of the study with respect the effect of lateral spreading on piles. The second stage of the tests which included 6 various experiments started in 2015 by design and built of a large laminar shear box and the tests were completed in 2021. The laminar shear box used in this research has outer dimensions of 4.2 m length, 2.4 m width and 2.0 m height and inner dimensions of 3.06 m length, 1.72 m width and 1.8 m height. Fig. 1 is an illustration of these two boxes. Zero height water sedimentation of Firuzkuh no.161 sand, a common soil in experimental studies in Iran, which is a clean uniformly graded sand with mean size of 0.24 mm, was used for modelling the liquefiable layer in both sets of studies. The main physical properties of Firuzkuh sand is outlined in Table 1.

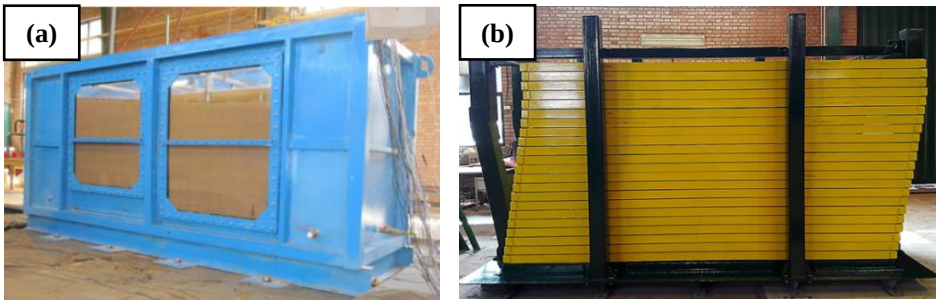

Fig. 1. (a): rigid box, (b): laminar shear box, designed and constructed for the reported studies

Table 1. Properties of Firuzkuh silica sand no. 161

Specific gravity	Mean grain size (D_{50}) (mm)	D_{10} (mm)	Maximum void ratio (e_{max})	Minimum void ratio (e_{min})	Coefficient of uniformity (C_u)
2.670	0.24	0.18	0.884	0.567	1.49

During this fairly long research, the effects of lateral spreading on a group of single piles and various pile groups with different configurations (e.g., 2×2, 3×3, 3×5, etc. with or without superstructure) were studied. The similitude law proposed by Iai [29] and Iai et al. [30] were used to calculate mechanical and geometrical properties of the piles in the models. In most of the reported experiments, the geometrical (prototype/model) scale was selected to be $\lambda=8$ and only the case studies are different. Model piles were designed based on JRA 2002 [8] to withstand the exerted lateral spreading forces. Aluminum pipes (T6061 alloy) and high density polyethylene (HDPE) pipes were used to similitude steel or concrete piles, respectively. In all models, the piles were sufficiently instrumented with pair strain gauges to detect pure bending moments at various sections. The soil at far field were also instrumented to

measure various parameters during and after shaking. Various parameters including acceleration and pore water pressure in different spatial positions of the free fields and near the piles, acceleration at the pile caps, surficial displacements, and bending moments in the piles were measured and evaluated. Also colored sands were formed in a grid pattern at surface of all models as well as in vertical columns at side of the rigid box models behind the Plexiglas windows. In order to monitor the lateral displacement of the soil during lateral spreading, digital high speed cameras and camcorders were implemented both at top and side of the models. In rigid box models the side cameras and camcorders could capture the lateral soil movements though the transparent windows provided especially for this purpose and in laminar shear box they could only record the box shape variation during the shakings. Input shaking consisted of 30 sinusoidal cycles with frequency of 3 Hz with two ramps of three cycles at the start and the end of shakings (Fig. 2). Acceleration amplitude of the input loading was 0.2g and 0.3g for the study of the effects of lateral spreading on piles. Also to study the effect of post liquefaction and post lateral spreading on piles several higher input motions were applied to each physical model. However, this part is not going to be covered in this paper.

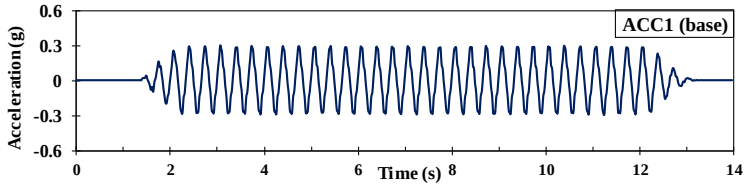

Fig. 2. Input motion applied to the physical models

3 Effects of Lateral Spreading on a Group of Single Piles

The first conducted experiment was on the investigation of the behavior of a group of piles without pile cap in a gently sloping liquefiable ground without a non-liquefiable crust. General test results including time-histories of accelerations, pore water pressures, displacements and bending moments have been presented by Haeri et al. [9]. It was found that the free field soil started to move laterally, right after being liquefied and kept moving towards the downslope until the end of the shaking, while the piles moved with the soil at the early stages of shaking, approaching a maximum displacement at the pile head and then bounced back gradually keeping a residual displacement at the end (Fig.3) The results indicated that lateral soil pressures exerted from laterally spreading ground vary in individual piles of a group depending on the pile position within the group (Fig. 4). In piles arranged in longitudinal direction, the downslope pile experienced less soil pressure comparing to the upslope one because of the shadow effect. In the transverse pile set, the middle pile received less pressure than the side piles as a result of neighboring effects. The behavior of piles in a group (without pile cap) located in a sloping ground far from a free face can be different from those located behind a quay wall or close to a free face. The reason could be the fact that in sloping ground, the lateral spreading starts from the upslope whereas in free face or quay wall cases the lateral spreading starts from the downslope. As a result, in sloping ground, the front pile is directly pushed by the laterally spreading

liquefied soil while the shadow pile is protected by the front pile against the direct impact of the liquefied soil hence experiencing less pressure comparing to the front pile. Therefore, the results revealed the importance of the effects of the pile position in the pile group.

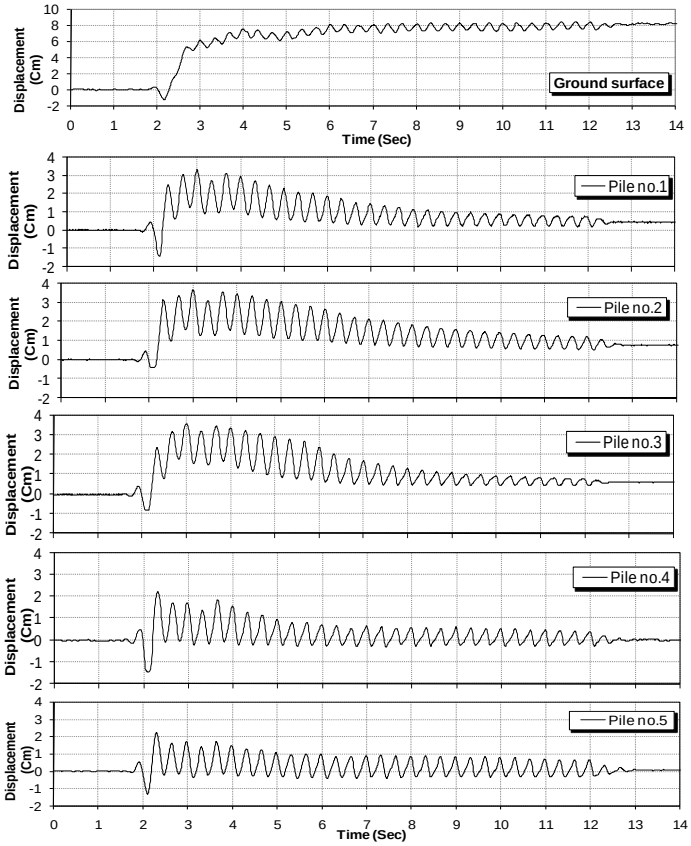

Fig.3. Time histories of ground surface displacement and lateral displacements of the pile heads [9].

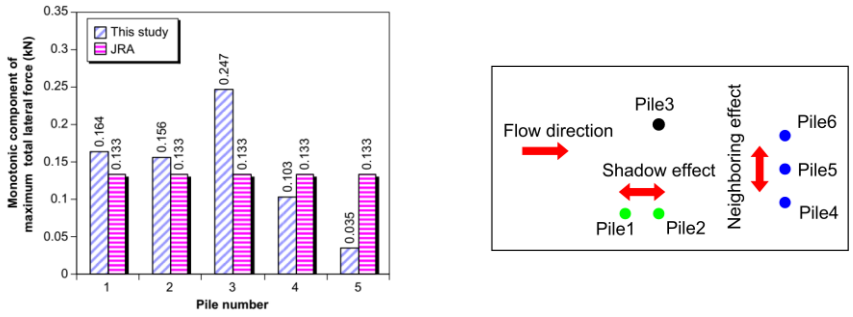

Fig. 4. Comparison between back-calculated monotonic component of maximum total lateral forces from shake table test on a group of single piles and JRA code [9].

In that research, the force-based and displacement-based methods were implemented to evaluate the bending moment profile of the single pile (i.e., Pile 3). Response of single piles to lateral spreading can be obtained by force based method in which the lateral pressures exerted on the piles are modeled as imposed limiting pressures similar to the procedure that JRA code [8] stipulates. This code specifies the induced lateral pressures as 30% of the total overburden pressure of liquefiable layer as shown in Fig. 5. Another procedure for the analysis of piles under lateral spreading is the displacement based approach in which a Beam on Nonlinear Winkler Foundation (BNWF) model is utilized. In the latter approach**,** as depicted in Fig. 5, the free field lateral soil displacement (Δ_{soil}) was applied at free ends of the p–y springs of the laterally spreading soil. In order to obtain the p–y curve for a liquefied or laterally spreading soil, a reduction factor which is known as p-multiplier is commonly applied to the corresponding p–y curve of the non-liquefied soil. In order to compare the capability of the two methods in predicting the behavior of the single pile in that experiment, bending moment diagram along the pile 3 was calculated based on each method and the results are plotted in Fig. 5. As shown in this figure, displacement based method using p-multiplier value of 0.064 proposed by Brandenburg [31] and p-multiplier value of 0.02 read from the lower bound curve suggested by AIJ [32] underestimate the bending moments in the pile. However, differences between measured and predicted bending moments by AIJ [32] method is much more evident in this regard. Moreover, using a best match p-multiplier value of about 0.115 which is equal to the upper bound value of Brandenburg [31] seems to be more capable of predicting the induced bending moment in the pile. Finally, as it can be observed in Fig. 5, force based approach based on JRA [8], predicted the maximum bending moment in the single pile to be about 45% of the monotonic component of that, recorded in the experiment.

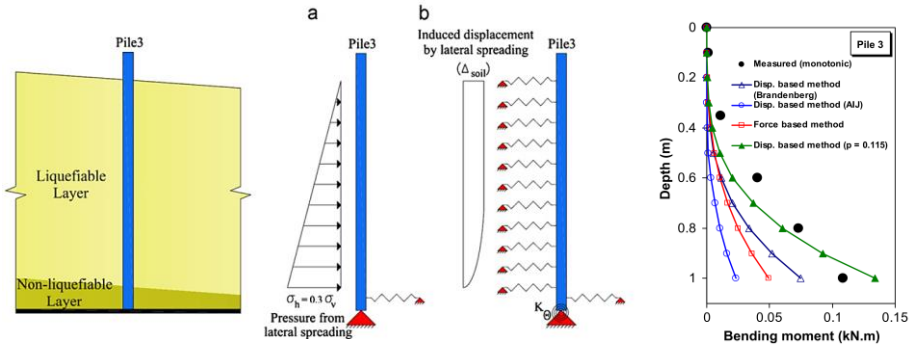

Fig. 5. Numerical modelling of a single pile under lateral spreading: (a) force based approach, (b) displacement based approach, and Comparison between measured and computed bending moments along the model pile [9]

4 Effects of Lateral Spreading on 2×2 pile groups

Different aspects of the behavior of 2×2 pile groups under liquefaction-induced lateral spreading in a medium dense liquefiable layer, located between a crust and bottom non-liquefiable layers, were investigated using the shake table and rigid box at the first stage. The employed physical model consisted of two separate 2 × 2 pile groups.

A lumped mass of 12 kg was attached to the cap of one of the pile groups in order to study the effects of superstructure on the response of the pile groups during lateral spreading. The results of this experiment showed that total lateral forces on the piles are influenced by the shadow effect as well as the superstructure mass attached to the pile cap. The presence of superstructure was found to intensify the negative bending moments in the piles. It was also found that the kinematic lateral forces exerted on the piles in the lower half of the liquefied layer are significantly larger than those recommended by JRA code [8] (Fig. 6). This observation can be attributed to the lateral displacement pattern of the soil which were obtained by analyzing the photos taken from the transparent side of the model (Fig. 6). As seen in this figure, the maximum permanent soil displacement was about 20 cm at the end of shaking which occurred near the middle of the liquefiable layer. The maximum lateral soil displacement in non-liquefiable crust layer, which was considerably smaller than the maximum displacement observed in the liquefiable layer, however, occurred at the ground surface. Based on the calculated contribution coefficients of lateral forces, in liquefiable layer, the upslope row of the piles carried larger lateral forces than the downslope one while in non-liquefiable crust layer, the downslope row experienced greater forces. However, contribution coefficient of total lateral force in upslope row was overally greater than that obtained for downslope row.

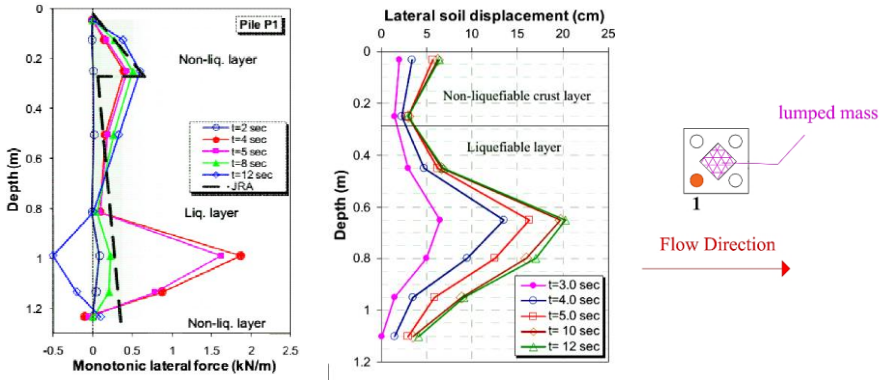

Fig. 6. Profile of kinematic component of the lateral forces on pile1 obtained from the model of 2×2 pile group, and profile of lateral soil displacement in free field at upslope side of the model extracted from snapshots during the shaking [16].

In next stage of the research, the effects of the existence of non-liquefiable crust layer on the responses of two sets of 2×2 pile groups to lateral spreading were studied using shake table and the large laminar shear box. The model without the crust layer consisted of a thick liquefiable layer with a relative density of 15% being underlain by a dense non-liquefiable layer. Time histories of the lateral displacement at the ground surface of the two models with and without crust layer are compared in Fig. 7. As seen in this Figure, existence of the non-liquefiable crust layer increased the maximum soil lateral displacement by 55%. This was in good agreement with the results of bending moments of the piles which showed that the bending moments of 2×2 piles increased significantly in the case of existence of the crust layer. Profiles of

bending moments on piles in the model with and without the crust layer and superstructure are exhibited in Fig. 8 and Fig. 9, respectively. According to these figures, existence of the crust layer and also existence of the lumped mass increase the maximum bending moment in the piles due to lateral spreading. Between these two parameters, the effect the existence of the crust layer on the responses of the piles is more remarkable.

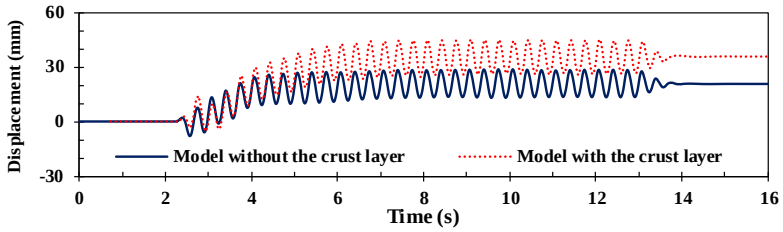

Fig. 7. Time histories of the free field soil displacement of the models with and without crust.

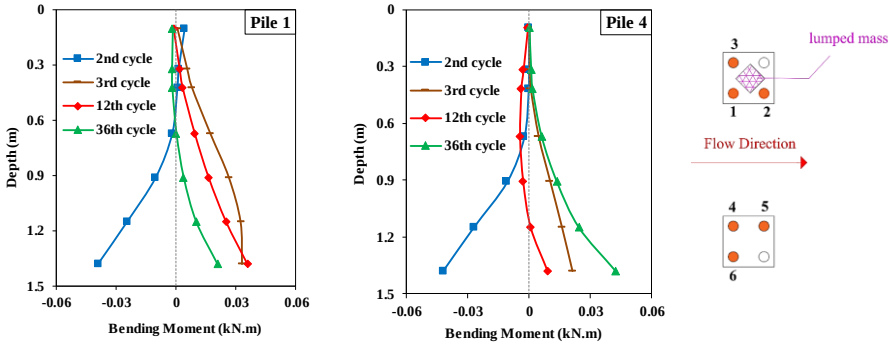

Fig. 8. Profiles of bending moments of the piles in the models with and without superstructure, without the crust layer tested in laminar box.

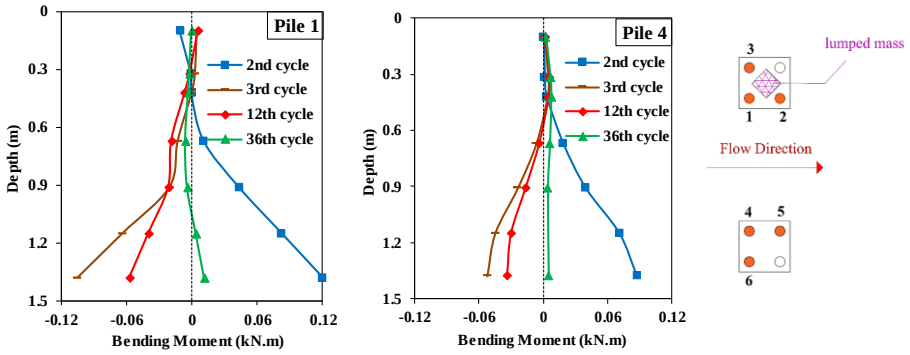

Fig. 9. Profiles of bending moments of the piles in the models with and without superstructure, with the crust layer tested in laminar box.

5 Effects of Lateral Spreading on 3×3 Pile Groups

The responses of a 3×3 pile group to liquefaction-induced lateral spreading was investigated using 1-g shake table test and the rigid box in the first stage of the study. The model ground consisted of a three layers soil profile including a base non-liquefiable layer, a middle loose liquefiable layer and an upper non-liquefiable crust layer. The results showed that lateral forces exerted by lateral spreading were not the same in the individual piles of the group, both in transverse and longitudinal directions, depending on the pile position within the group. Monotonic components of maximum total lateral for on the piles were calculated by integrating the lateral soil pressures along the piles. These total lateral forces were separately evaluated for the liquefied layer and the non-liquefiable crust. The calculated forces are displayed in Fig. 10. According to this figure, the amount of total lateral force in pile P2 (located in middle row) is less than the piles located in upslope and downslope rows, i.e. piles P1 and P3. Total lateral force on pile P1 is about 1.24 times that exerted on pile P2. This occurs due to the shadow effect. Since the upslope pile is directly pushed by the laterally spreading soil and acts as a barrier for pile downslope pile, P2. Total lateral force exerted on pile P3 is the largest among all the other piles. Total lateral force on pile P3 is about 1.43 and 1.76 times those of piles Pl and P2, respectively. This can be described by the separation of soil from the downslope side of pile P3 during lateral spreading resulting in lack of lateral support. Comparing total lateral forces in pile Pl (the middle pile in upslope row) and P4 (the side pile in upslope row) shows that the side pile receives larger force than the middle pile by a factor of about 1.27. This phenomenon is called neighboring effect. It was also found that the magnitude of lateral pressure due to lateral spreading on the 3×3 pile group of this study, in average, is close to the values recommended by the JRA design code (Fig. 11).

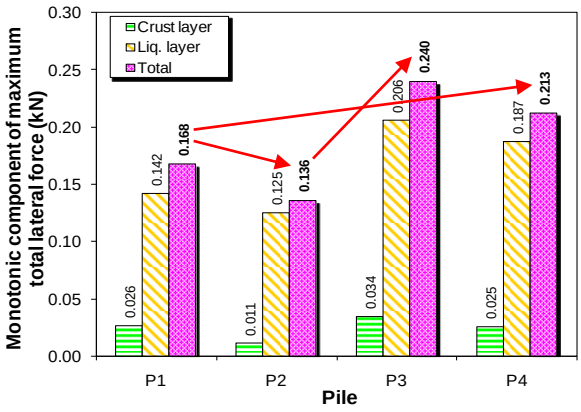

Fig. 10. Comparison of maximum total lateral forces on different piles of the 3×3 group in rigid box [11].

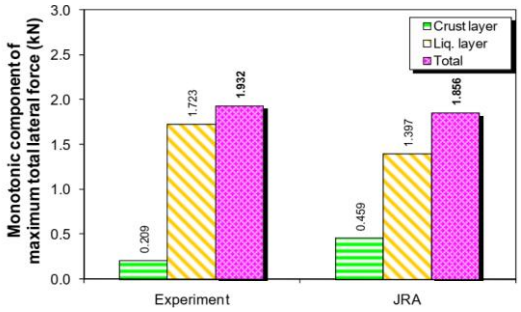

Fig. 11. Comparison between monotonic components of maximum total lateral forces in pile group of this experiment and JRA 2002 recommended values [11].

In the second stage of the experiments, the laminar shear box was employed in physical modelling a 3×3 pile group in a gently sloped ground. All the properties of these two models designed and constructed the same except the containers. Bar charts of the maximum kinematic lateral forces on the piles due to lateral spreading are presented in Fig. 12. The maximum lateral force on pile 2 was shown differently in Fig. 12, because the lateral force applied on pile 2 was interpolated from other piles as strain gauges attached to this pile were not enough to be conclusive. As seen in Fig. 12, the kinematic lateral forces of side piles (i.e., piles 1, 2 and 3) are more than corresponding piles in the middle row, i.e. piles 4, 5 and 6, respectively. This issue can be attributed to neighboring effects. Also the downslope piles experienced more kinematic forces due to lateral spreading compared to those in the upslope row of the group. For example, the maximum kinematic lateral force on pile 1 was about 81% higher than that for pile 3. This can be attributed to a more lateral movement of the soil at downstream of the model.

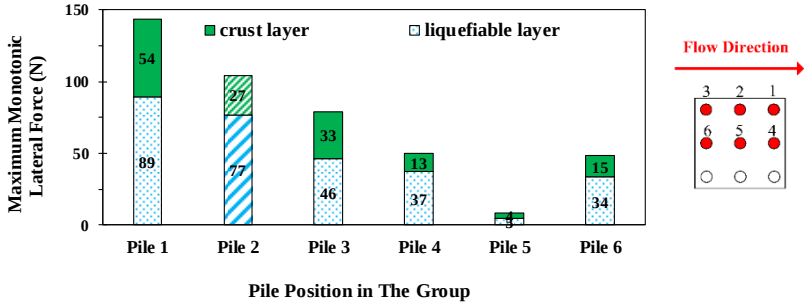

Fig. 12. Bar chart of maximum monotonic lateral forces on different piles of a 3×3 pile group tested in laminar shear box.

Maximum monotonic lateral force on the pile group in this experiment was also compared with the values proposed by JRA design code [8] as seen in Fig. 13. According to this figure, the maximum monotonic lateral force obtained in this experiment using laminar shear box, unlike the test results for rigid box, is significantly lower than that estimated by JRA code. Considering the results obtained by two containers it can be assumed that the forces suggested by JRA can be assumed as an upper bound for kinematic force induced by lateral spreading on 3×3 piles of a pile group.

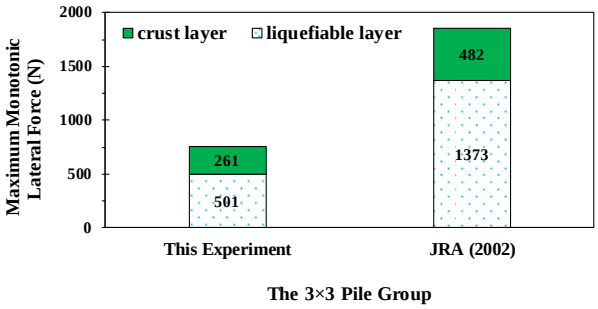

Fig. 13. Bar chart of the maximum kinematic lateral force due to lateral spreading on the pile the 3×3 pile group tested in laminar shear box.

6 Effects of Boundary Conditions on Physical Modelling Results

The effects of boundary conditions of the physical models on the results of the experiments using shake table were investigated by comparing the results of two identical experiments with different containers, the rigid box and the laminar shear box as discussed above. The differences between the obtained results of these two experiments can only be attributed to the effect of boundary conditions. It was found that the responses of the model in the rigid box is higher due possibly to wave reflections from the rigid walls and also bouncing back of the liquefied soil from rigid boundaries. For example, time histories of the ground lateral displacement at free filed for these two models are exhibited in Fig. 14. According to Fig. 14 the maximum and final (residual) soil displacement at free field in the rigid box, are about 20% and 40% are more than those of laminar shear box, respectively. This is in good agreement with the results of the bending moments generated in the piles. Time histories of the bending moment of the upstream pile for the models using rigid and laminar shear boxes are compared in Fig. 15. The maximum bending moment of this pile in the model with rigid box was about 2.7 times of that in the other model.

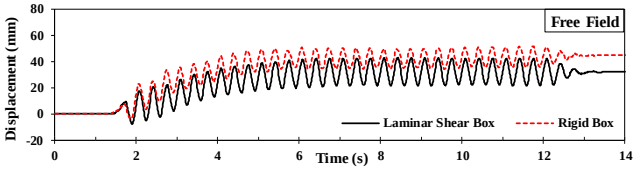

Fig. 14. Time histories of surface displacements in the models using rigid and laminar shear boxes [10].

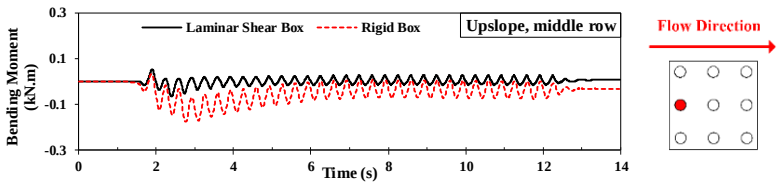

Fig. 15. Time histories of the bending moments of the upstream pile in the models using rigid and laminar shear boxes.

7 Case Studies of Lateral Spreading Effects on Pile Groups

Two physical modelling were carried out to model real cases to study the effect of lateral spreading on two different pile groups, one using rigid box and the other implementing laminar shear box as are introduced and discussed briefly in the following.

7.1 Dolphin-Type Berth

The effects of liquefaction-induced lateral spreading on 3 piles of a dolphin-type berth were investigated using 1-g large scale shake table and the rigid box in stage 1 of these studies. Due to the size of the berth and the box the scaling factor was chosen to be 20. The soil profile included a 1.2 m thick liquefiable layer (loose sand with relative density of 15%) overlying a bottom non-liquefiable dense sand layer having maximum thickness of 25 cm and relative density of about 80%. All the soil layers were inclined by 7% towards downslope. The results indicated that large bending moments were induced in the piles due to lateral spreading. Also the downslope piles of the group received greater bending moments than the upslope one. In upper half of the liquefiable layer, where the soil fully liquefied (r_u = 1.0), substantial active lateral pressures were exerted on the piles while in the lower half, in which the soil did not liquefy (r_u = 0.5), a passive pressure zone was developed. In Fig. 16, a comparison is made between the maximum monotonic component of lateral soil pressure on model piles and the lateral soil pressure calculated based on JRA code [8]. As shown in Fig. 16, the magnitude and pattern of the lateral pressures on Pile 3 are rather consistent with the prediction of JRA code up to a depth of about 0.6 m corresponding to the upper half of the pile and liquefiable layer. The inconsistency observed in lower depths can be attributed to the fact that the prediction of JRA code was based on the assumption that the lateral soil movement occurred in whole depths of the liquefiable layer. However, smaller lateral soil movement in lower depths created a passive pressure zone in these depths during the experiment. Another finding is that the pattern of lateral soil pressure distribution along the upslope pile (i.e. pile P1) is different from what observed for the downslope one (i.e. pile P3).

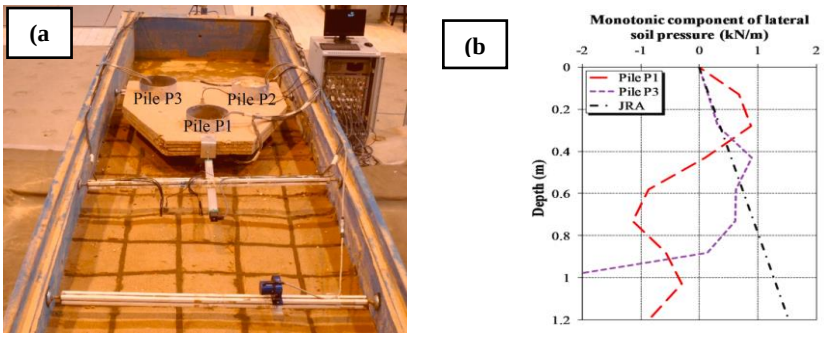

Fig. 16. a): Top view of the physical model of dolphin- type berth on SUT shaking table, b): profiles of monotonic component of maximum lateral soil pressure on model piles along with the corresponding values recommended by JRA design code [14, 17].

7.2 Deep Foundation of a Bridge

The behavior of the deep foundations of Nahang-e-Roogah bridge, a bridge near Bandar-e-Anzali city in North Iran, along Caspian see was studied. For this purpose, a shake table test using laminar shear box with scaling factor of 20 was conducted to study the dynamic response of a 3×5 pile group subjected to liquefaction induced lateral spreading in the second stage of the experiments. The results showed that the location of the piles in the group was important. According to Fig. 17, the upslope position of the pile group experienced greater bending moments than downstream piles. This can be attributed to the effects of flow direction in lateral spreading which is known as the "shadow effects". The results also showed that the maximum acceleration of the pile cap amplified being twice the input acceleration amplitude. This is a notable result for design of a superstructure in a liquefiable soil-pile system.

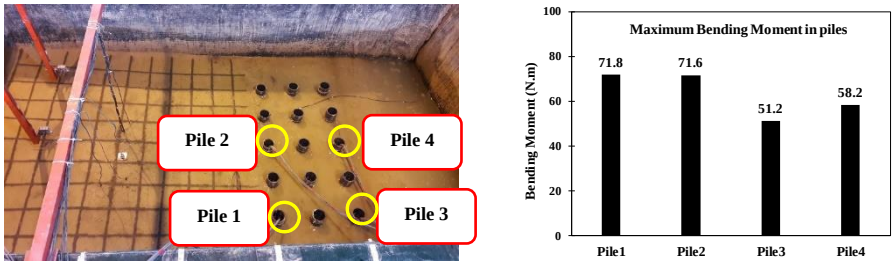

Fig. 17. Top view of physical model of 3×5 pile group of Nahang-e-Roogah Bridge, and bar graph of maximum amounts of bending moment of the piles [15].

8 Assessment of Mitigation Methods Against Lateral Spreading

In this research, effectiveness of some mitigation methods (e.g., stone column, micropile) against lateral spreading were investigated using 1-g shake table tests. Main aspects of these models are briefly presented and explained in the following.

8.1 Assessment of Stone Column Method

The effectiveness of stone columns as remedial measures against lateral spreading in a 3×3 flexible pile group was investigated by conducting shake table tests using rigid box in first round of the conducted research. In order to evaluate the performance of employed stone columns, comparisons were made between profiles of bending moments in individual piles of the groups obtained for mitigated and unmitigated cases. The stone columns were installed at upslope and downslope sides of the pile group after preparation of one of the unmitigated models (Fig. 18). Construction of the stone columns caused densification of the loose liquefiable layer and associated vertical settlements in an area of about 1.5 meters in length extending over the upslope and downslope sides of the stone columns. All settlements were carefully measured after construction of the stone columns and associated volume decrease was subsequently determined to calculate the new relative density of the sand layer which was estimated to change from 15% to about 65% in the affected zone, indicating a reduction in liquefaction potential and subsequent lateral spreading in that area.

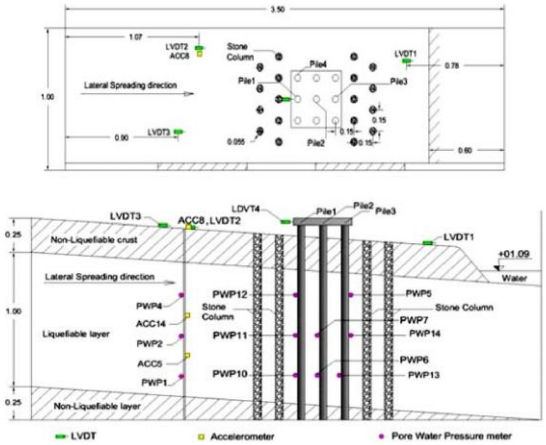

Fig. 18. Plan and cross section views of the physical model along with the stone columns [22].

Bending moments in piles increased significantly due to lateral spreading in unmitigated model. However, after a peak, due to the loss of shear strength in liquefied soil and rigidity of the piles, the pile groups bounced back towards the upslope shaking continued. Accordingly the bending moments in the piles decreased up to the end of shaking. However, in the model with stone columns, bending moments at different elevations of the pile continuously increased during the shaking, due to higher density of the soil and its resistance against elastic rebound of the piles. Therefore the residual bending moments in the piles at the end of the shaking were significant, while the maximum bending moments in the piles slightly showed increase. In fact, during the shaking and lateral pressure exerted by lateral spreading in upstream part of the model to the mitigated zone including pile groups, each cycle of the shaking caused a minor slide in the mitigated ground towards downslope, imposing incremental lateral pressures on the piles similar to the behavior of soils during cyclic mobility compared to the liquefaction and associated lateral spreading around the piles in unmitigated case. As a result, the pile group moved along with the soil towards the downslope so its deflection increased progressively by each loading cycle, leaving a residual lateral displacement as well. However, if the earthquake and associated number of cycles are limited, the stone column can be effective. For instance, during an earthquake with a magnitude of Mw = 6.6 (7 cycles of shaking), stone columns could reduce the maximum bending moment of a critical pile in the group, by about 80%. As the magnitude of earthquake and associated number of cycles increased, the effectiveness of the prepared stone columns with such a configuration and method, decreased. Hence, the results showed that the constructed stone columns could effectively reduce the bending moments in piles due to lateral spreading up to a particular level of earthquake magnitude. A series of shake table experiments were also conducted on two set of 2×2 pile groups (with and without superatructure) in the laminar shear box, in the second stage of the study, to investigate the efficacy of stone column technique as a mitigation method against liquefaction-induced lateral spreading and compared the behavior of pile groups in treated and untreated liquefiable layers. In one of the models, 29 stone columns with a

diameter of 60 cm at prototype scale and triangular configurations were constructed. The stone columns technique can combine the beneficial effects of densification, reinforcement, and increased drainage of excess pore water pressure. In the study, the stone columns were constructed in a way to minimize densification of the surrounding soil, for observing mainly the drainage and some reinforcement effects of stone columns on liquefaction induced lateral spreading and its effects on the studied pile groups. The results illustrated that stone column technique prepared in this method significantly decreassed lateral displacemnts in the free field and bending moments in the piles, while increased the accelearions in the pile caps and rate of dissipation of excess pore water pressure in the liquefiable layer. Bar charts of the maximum bending moments in the piles of treated and untreated models are presented in Fig. 19. As seen in this figure, stone columns reduced the maximum bending moments of the piles between 51% to 77% in this case.

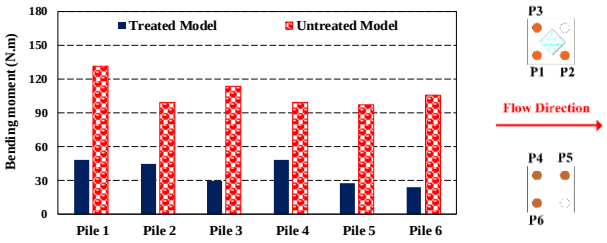

Fig. 19. Bar charts of the maximum bending moments of the piles in treated and untreated models with stone columns [24].

8.2 Assessment of Micropile Method

Effectiveness of a micro-pile system as a countermeasure for the effect of lateral spreading on piles was evaluated using 1g shake table and the rigid box model tested on a 3×3 flexible pile group. For this purpose, two physical models including a benchmark model without any mitigation measure and a model remediated with micro-piles were constructed and tested in the first stage of the research. It should be noted that polypropylene pipes were used as model micropiles which were inserted into the liquefiable and the bottom non-liquefiable layers with a spacing of 7.5 cm (center to center) after construction of the physical model. In general, the results of the shake table tests on these models showed that the micropile system deployed in that research did not considerably reduce the kinematic lateral force as well as the induced bending moments due to lateral spreading on the pile group. Besides, the accelerations recorded on the pile cap were adversely amplified compared to the case where no mitigation measure is adopted. The employed micropiles were able to reduce the soil pressure exerted by the upper non-liquefiable layer on the upslope piles of the group. However, they did not effectively decrease the lateral pressures exerted by liquefiable layer on the piles. The soil displacement in the upper parts of the model remediated with micropiles was generally smaller than that in the model with no mitigation measure. This explains that the employed micropiles restricted the lateral displacement of the upper non-liquefiable layer and partially that of the upper depths of the liquefiable layer. However, this restriction was not noticeable in deeper

depths of the liquefiable layer. Employing the micropiles in a tighter pattern, adopting stiffer ones or fixing them in the underlying non-liquefiable layer may be considered to more effectively restrict the lateral movement of the liquefied soil thus to reduce the lateral soil pressure on piles subjected to lateral spreading. However, effectiveness of the mentioned solutions needs further investigations in future.

9 Possible Sources of Errors in Physical Modelling

Errors involved in physical modelling can be divided into three main categories: system errors, human errors and environmental errors. The system errors are associated with the errors involved in measuring sensors, data acquisition system (DAS) and the main shaking system. The main shaking system is a high precision 280 bar Instron-Schenck system with a high definition control system which is completely isolated from any virus or intrusion. In the tested physical models it has been delicately tried to minimize errors involved in the measuring sensors by choosing high accuracy sensors and calibrated or checked them against the reference sensors. Also it was tried to minimize the noise associated with the data in the DAS. Some of the errors which may be encountered is due to the installing method of the sensors in which both the human and environmental errors may be involved. For instance very small rotation or dislocation in accelerometers during installation or during shaking and liquefaction or lateral spreading may affect the recorded accelerations. The solution for minimizing this error might be installing the accelrometers on a base with a relatively large area. In addition, strain gauges are very sensitive to temperature and water. To solve the water problem, waterproof sensors should be used or water resistant epoxies should be implemented. Temprature change may affect on the measured data by strain gauges which is an environmental error and erronous result may be deducted. The effect of temperature on strain gauges can be diminished automatically by using half way Watson Bridges. This technique have been used in installationo of strain gauges on all piles in this study. The non-uniformity of the loose sandy layer is another source of error for which a special hopper was designed, constructed and used for water sedimentation of the loose sandy layers in construction of the physical models.

10 Conclusion

Liquefaction-induced lateral spreading can cause severe damages to deep foundations. Two stages of physicsl modelling including several large scale 1-g shake table tests, using both rigid and laminar shear boxes, which have been deployed for investigating various aspects of the effects of lateral spreading on single and pile groups with different configurations of piles, soil profiles and superstructures have been reported and discussed briefly in this paper. Also some conducted experiments to assess the efficacy of different mitigation methods against the effect of lateral spreading on a number of pile groups have been introduced and explained shortly. The results indicated that dynamic soil-pile interactions in liquefied and laterlly spreading grounds are complex problems which can be affected by numerous parameters. Hence, althogh some general results might be deducted from the observations and test results, however, each problem should be solved according to its geometrical and mechanical

characteristics of the soil layers and the piles. Therefore, further experiments and numerical studied are still required.

Acknowledgment

The partial financial supported by Construction and Development of Transportation Infrastructures Company and the partial financial support by Transportation Research Institute, Ministry of Roads & Urban Development of Iran for conducting the studies reported in this paper are acknowledged. Also the partial financial support granted by Research Deputy of the Sharif University of Technology is acknowledged. The experiments were conducted at Shake Table Facilities of Civil Engineering Department, Sharif University of Technology. The contribution of all faculty, graduate students and technicians in performing the experiments is acknowledged as well.

References

1. Hamada, M., Isoyama, R., Wakamatsu, K.: Liquefaction Induced Ground Displacement and Its Related Damage to Lifeline Facilities. Soils and Foundation, January (Special Issue), 81–97 (1996).
2. Hamada, M., Yasuda, S., Isoyama, R., Emoto, K.: Study on Liquefaction-Induced Permanent Ground Displacements. Association for the Development of Earthquake Prediction, Japan (1986).
3. Tokimatsu, K., Mizuno, H., Kakurai, M.: Building Damage Associated with Geotechnical Problems. Soils and Foundations, January (Special Issue), 219-234 (1996).
4. Tokimatsu, K., Asaka, Y.: Effects of Liquefaction-Induced Ground Displacements on Pile Performance in The 1995 Hyogoken–Nambu Earthquake. Special Issue of Soils and Foundations, 163-177 (1988).
5. Bardet, J. P., Kapuskar, M.: Liquefaction Sand Boils in San Francisco During 1989 Loma Prieta Earthquake. Journal of Geotechnical and Geoenvironmental Engineering 119(3): 543-562, (1993).
6. Bhattacharya, S., Sarkar, R., Huang, Y.: Seismic Design of Piles in Liquefiable Soils. In: Huang Y., Wu F., Shi Z., Ye B. (eds) New Frontiers in Engineering Geology and the Environment, Berlin, Heidelberg: Springer Geology. Springer (2013).
7. Tamura. K.: Seismic Design of Highway Bridge Foundations with The Effects of Liquefaction Since the 1995 Kobe Earthquake. Soils and Foundations 54(4), 874-882 (2014).
8. Japan Road Association (JRA): Seismic Design Specifications for Highway Bridges. English version, Prepared by Public Works Research Institute (PWRI) and Ministry of Land, Infrastructure and Transport, Tokyo, Japan (2002).
9. Haeri, S. M., Kavand, A., Rahmani, I., Torabi, H.: Response of A Group of Piles to Liquefaction-Induced Lateral Spreading by Large Scale Shake Table Testing. Soil Dynamics and Earthquake Engineering 38, 25-45 (2012).
10. Haeri, S. M., Rajabigol, M., Salaripour, S., Kavand, A., Sayaf, H., Afzalsoltani, S., Pakzad, A.: Effects of Liquefaction-Induced Lateral Spreading on a 3×3 Pile Group Using 1g Shake Table and Laminar Shear Box. Proceedings of the 7th international conference on Earthquake Geotechnical Engineering, Rome, Italy (2019a).
11. Haeri, S.M., Kavand, A., Asefzadeh, A., Rahmani, I.: Large Scale 1-g Shake Table Model Test on The Response of a Stiff Pile Group to Liquefaction-Induced Lateral Spreading, Proceedings of the 18th International Conference on Soil Mechanics and Geotechnical Engineering, Paris, France (2013).
12. Haeri, S. M., Rajabigol, M., Salaripour, S., Sayaf, S., Pakzad, A., Kavand, A.: Study of Dynamic Response of a 3×3 Pile Group to Liquefaction-Induced Lateral Spreading Using Shake Table, Proceedings of 4th national conference on Geotechnical Engineering, Tehran, Iran, in persian (2019b).

13. Haeri, S. M., Rajabigol, M., Sayaf, H., Salaripour, S., Seyed Ghafouri, S. M. H., Kafashan, F., Khoshnoud, A.: Response of 2×2 Pile Groups to Soil Liquefaction in Inclined Base Layer: 1g Shake Table Tests, Proceedings of 8th international conference on Semiology & Earthquake Geotechnical Engineering, Tehran, Iran (2019c).
14. Haeri, S. M., Kavand, A., Raisianzadeh, J., Padash, H., Rahmani, I., Bakhshi, A.: Observations from a Large Scale Shake Table Test on a Model of Existing Pile-Supported Marine Structure Subjected to Liquefaction Induced Lateral Spreading, Proceedings of the 2nd European Confrence on Earthquake Engineering and Seismology, Istanbul, Turkey (2014).
15. Haeri, S. M., Rajabigol, M., Moradi, M., Zangeneh, M.: A Case Study of Dynamic Response of a 3×5 Pile Group to Liquefaction induced lateral spreading: 1-g Shake Table Test. Proceedings of the 12th International Congress on Civil Engineering, Mashhad, Iran (2021).
16. Kavand, A., Haeri, S. M., Asefzadeh, A., Rahmani, I., Ghalandarzadeh, A., Bakhshi, A. : Study of the Behavior of Pile Groups During Lateral Spreading in Medium Dense Sands by Large Scale Shake Table Test. International Journal of Civil Engineering 12(3), 374-39 (2014).
17. Kavand, A., Haeri, S. M., Raisianzadeh, J., Sadeghi Meibodi, A., Afzal Soltani, S.: Seismic Behavior of A Dolphin-Type Berth Subjected to Liquefaction Induced Lateral Spreading: 1g Large Scale Shake Table Testing and Numerical Simulations. Soil Dynamics and Earthquake Engineering 140, (2021).
18. Su, L., Tang, L., Ling, X., Liu, C., Zhang, X.: Pile Response to Liquefaction-Induced Lateral Spreading: A Shake-Table Investigation. Soil Dynamics and Earthquake Engineering 82, 196-204 (2016).
19. Ebeido, A., Elgamal, A., Tokimatsu, K., Abe, A.: Pile and Pile-Group Response to Liquefaction-Induced Lateral Spreading in Four Large-Scale Shake-Table Experiments, Journal of Geotechnical Geoenviromental Engineering 145(10), (2019).
20. He., L., Elgamal., A., Hamada., M., Meneses, J.: Shadowing and Group Effects for Piles During Earthquake-Induced Lateral Spreading, Proceedings of the 14th World Conference on Earthquake Engineering, Beijing, China (2008).
21. Seed, H. B., Booker, J. R.: Stabilization of Potentially Liquefiable Sand Deposits Using Gravel Drains. Journal of Geotechnical and Geoenvironmental Engineering 103(7), 757–768 (1977).
22. Kavand, A., Haeri, S. M., Raisianzadeh, J., Padash, H., Ghalandarzadeh, A.: Performance Evaluation of Stone Columns as Mitigation Measure Against Lateral Spreading in Pile Groups Using Shake Table Tests. International Conference on Ground Improvement and Ground Control (ICGI 2012), Paris, France (2012).
23. Kavand, A., Haeri, S. M., Raisianzadeh, J., Afzalsoltani. S.: Effectiveness of A Vertical Micropile System for Mitigation of Liquefaction-Induced Lateral Spreading Effects on Pile Foundations: 1g Large Scale Shake Table Tests. Scientia Iranica (2021).
24. Haeri, S. M., Rajabigol, M., Zangeneh, M., Moradi, M.: Assessment of Stone Column Technique as a Mitigation Method Against Liquefaction-Induced Lateral Spreading Effects on 2×2 Pile Groups. Proceedings of the 4th International. Conference on Performance-based Design in Earthquake. Geotechnical Engineering (PBD-IV) in Beijing, China (2022).
25. Elgamal, A., Lu, J., Forcellini, D.: Mitigation of Liquefaction-Induced Lateral Deformation in a Sloping Stratum: Three-dimensional Numerical Simulation. Journal of Geotechnical and Geoenvironmental Engineering 135(11), 1672-1682 (2009).
26. Foellini, D., Tarantino, A. M.: Assessment of Stone Columns as a Mitigation Technique of Liquefaction-Induced Effects during Italian Earthquakes (May 2012), Hindawi Publishing Corporation, The Scientific World Journal, (2014).
27. Tang, E., Orense, R. P.: Improvement Mechanisms of Stone Columns as A Mitigation Measure Against Liquefaction-Induced Lateral Spreading. New Zealand Society for Earthquake Engineering, Aukland (2014).

28. Liu, J., Kamatchi. P., Elgamal. A., Using Stone Columns to Mitigate Lateral Deformation in Uniform and Stratified Liquefiable Soil Strata, International Journal of Geomechanics 19(5), (2019).
29. Iai, S., Similitude for Shaking Table Tests on Soil–Structure–Fluid Model in 1g Gravitational Field, Soils and Foundations, 29(1): 105-118, (1989).
30. Iai, S., Tobita, T., Nakahara, T.: Generalized Scaling Relations for Dynamic Centrifuge Tests. Géotechnique 55(5), 355-362 (2005).
31. Brandenburg, S. J.: Behavior of Pile Foundations in Liquefied and Laterally Spreading Ground. PhD thesis, University of California at Davis, CA (2005).
32. Architectural Institute of Japan (AIJ): Recommendations for Design of Building Foundations (in Japanese), (2001).